Cryo-TEM imaging of a novel microemulsion system of silicone oil with an anionic/nonionic surfactant mixture

Lukas Wolf,[a] Heinz Hoffmann,*[a] Yeshayahu Talmon,[b] Takashi Teshigawara[c] and Kei Watanabe[c]

Received 3rd March 2010, Accepted 1st August 2010
DOI: 10.1039/c0sm00049c

We report the nanostructures in a novel microemulsion system of silicone oil, water and a surfactant mixture of an anionic and a nonionic surfactant. The phase diagram of the investigated system exhibits two isotropic single-phase channels for constant temperature. The upper channel, that is the channel with the higher mass fraction of nonionic surfactant, starts with an L_3-phase at the water side, and passes through a minimum continuously to the oil side. The channel with the lower mass fraction of nonionic surfactant starts with an L_1-phase at the water side, and passes with increasing oil content and increasing mass fraction of nonionic surfactant to the middle of the phase diagram and ends there. No connection between the two channels was detected at a surfactant concentration of 15%. The two channels are separated by a single L_α-phase and multiphase regions. In contrast to the results from microemulsions with nonionic surfactants, cryo-TEM micrographs on this system show that the upper phase channel has a bicontinuous structure from zero to only about 35% of oil. At higher oil content the channel contains water droplets in a continuous oil phase. At a water/oil ratio of 1 : 1, the structure looks like a polyhedral foam structure or a high internal phase emulsion (HIPE) structure, and not like the usual bicontinuous structure, as generally assumed. Nevertheless, the dimensions of the imaged bicontinuous and water-in-oil-structures were consistent with the theoretical consideration for nanostructures in microemulsions. The lower channel with its o/w-structure could not well be imaged with the cryo-TEM method. Instead of small droplets, small vesicles were imaged, that obviously were formed by the loss of oil in the thin film during the specimen preparation process for cryo-TEM.

Introduction

Microemulsions are thermodynamically stable phases of oil, water and surfactants.[1] Two types of microemulsions can be distinguished on the basis of the used surfactants, ionic surfactant microemulsions and nonionic surfactant microemulsions. Only a few microemulsion systems of ionic surfactants, where the ionic charge has not been shielded by excess salt, have been studied.[2,3] The best known system is probably the one of dodecane, water and didodecyldimethylammoniumbromide (DDAB). In the triangular phase diagram the system contains a large single-phase area. Surfactant concentrations of more than 10% are needed to produce single-phases from equal amounts of oil and water. The single-phase region has been studied in detail by different techniques. It contains regions with different macroscopic properties, *e.g.* viscous and non-viscous, conducting and not conducting regions.[4,5] In this system it is not possible, at constant surfactant concentration, to pass from the single aqueous phase to the oil phase without crossing phase boundaries. The situation in that respect is very different from microemulsions of nonionic surfactants.[6,7] Those systems usually contain a single-phase channel which reaches from the water side to the oil side of the phase diagram.[8] However, the temperature has usually to be varied to remain in the single-phase channel. These types of systems have been well studied, and their behaviour and the microscopic structures in the single-phase channel are known and well understood.[7] The occurrence of the single-phase channel has to do with the change of the amphiphilic properties with temperature. With increasing temperature the curvature of the amphiphilic monolayer changes from convex, to flat, to concave. As a consequence the microemulsion structures change, from the water side, from small oil droplets in water, to bicontinuous structures in the middle of the phase diagram, to w/o droplets on the oil side. The interfacial tension between the oil and the water is a sensitive parameter for the change of curvature.[9] Optimum solubilisation of oil in an aqueous surfactant solution is obtained at the minimum of the interfacial tension of the surfactant.

A change of the interfacial tension of a surfactant can also be brought about by adding a co-surfactant to the surfactant solution.[10] In the present investigation we chose therefore a binary mixture of a hydrophilic surfactant with a lipophilic surfactant. We hoped that by changing the mass fraction of two molecules it would be possible to find a single-phase channel for constant temperature. For the ionic surfactant we chose Ca^{2+} or Mg^{2+}-salts of SDS, and for the lipophilic co-surfactant we used iso-tridecyl-triethyleneglycolether (IT 3). It is commercially produced and is worldwide available under the name "Marlipal O13/30" like other well-known nonionic surfactants like Triton X 100.[11] The compound has a polydisperse distribution of EO-groups with average 3 EO-units.

By changing the mass fraction of the two molecules in the surfactant solution, it turned out to be possible to pass from an

[a]*University of Bayreuth, BZKG/BayKoll, Gottlieb-Keim-Str. 60, D-95448 Bayreuth, Germany. E-mail: heinz.hoffmann@uni-bayreuth.de*
[b]*Department of Chemical Engineering, Technion-Israel Institute of Technology, Haifa, 32000, Israel*
[c]*Shiseido Research Center, 2-2-1 Hayabuchi, Tsuzuki-ku, 224-8558, Japan*

L_1-phase with only $Ca(DS)_2$ over an L_α and an L_3-phase with the surfactant mixtures to an L_1/L_2 two phase situation for the solution with pure IT 3.[12] Some nonionic surfactants show the same sequence of phases with increasing temperature.

Results and discussion

Phase diagram of $Ca(DS)_2$/IT 3–H_2O/M_2

The plot of the surfactant mixture against the mass fraction x of oil between $x = 0$ and $x = 1$ is shown in Fig. 1. As oil, we chose the short silicone oil hexamethyldisiloxane (M2). The total surfactant concentration was kept constant at 15% (w/w), and the temperature at 40 °C (for details see ref. 12).

The phase diagram contains two isotropic single-phase channels, a lower one and an upper one. The upper one begins on the axis with the mass fraction of IT 3 at the L_3-phase. With increasing oil concentration, the channel first shifts to a lower IT 3 ratio and then again to a higher IT 3/$Ca(DS)_2$ ratio for higher oil ratios. It ends on the oil side with pure IT 3.

The lower channel begins at the water side on the phase boundary to a two phase L_1/L_α-region, and ends in the middle of the phase diagram at an IT 3 ratio of 0.65. We did not find a connection of the two channels.

For an IT 3 ratio of 0.7 we found two isotropic samples with increasing oil, one at 2% of oil and one at 25% of oil.

It is furthermore noteworthy that the L_α-phases of the $Ca(DS)_2$/IT 3 mixtures can solubilise large amounts of oil without breaking down. With the mass fraction of IT 3 $x = 0.55$ in the surfactant mixture it is possible to solubilise the same amount of oil as surfactant. Samples with x IT 3 = 0.55 and increasing amount of oil are shown in Fig. 2.

The L_α-phase, which is stable up to 15% of oil, is transformed with 20% oil into a two-phase system, and with 30% of oil finally into the single microemulsion phase.

The microemulsions in the lower channel are transparent phases with low viscosity, which show no flow birefringence under shear. The samples in the upper phase channel have somewhat different properties. The samples are not as transparent as samples from the lower channel. The samples look somewhat bluish, and their scattering intensity increases continuously from the water side to the middle of the phase diagram. For higher oil content the samples are transparent again. Pictures of samples from the lower and upper single-phase channel are shown in Fig. 3.

The different apparent macroscopic properties in the upper and lower phase channel for the same amount of oil are an indication that the structures in the two single-phase channels are different. The conductivity measurements in both single-phase channels, which are shown in Fig. 4, underline this assumption. For the lower channel (Fig. 4B), the conductivities decrease linearly with the oil content to the middle of the phase diagram, which is where the channel ends. The reason for the decrease is mainly the decreasing mass fraction of $Ca(DS)_2$. The conductivities therefore indicate that the microstructure in the lower channel does not change, and that the channel consists of a continuous water phase in which oil droplets are dispersed. The situation is very different in the upper single-phase channel (Fig. 4A), where the conductivity drops for a few percent of oil (5%) to only about 18% of its value in the L_3-phase, even though the fraction of $Ca(DS)_2$ is increasing from 23% to 35%. The conductivities there indicate a dramatic change in the nanostructure of the bi-continuous channel with solubilisation of small amounts of oil into the L_3-phase. Obviously the constraints

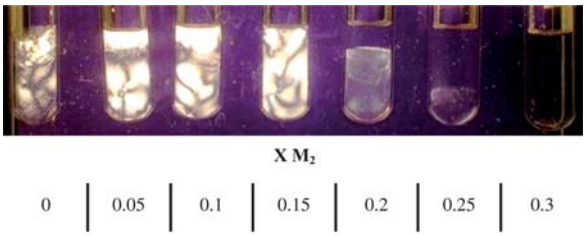

Fig. 2 Samples with constant 15% (w/w) surfactant mixture $Ca(DS)_2$/IT 3, mass fraction x IT 3 = 0.55, and increasing mass fraction x of silicone oil M_2 in the solvent at 40 °C, photographed in between crossed polarisers. Single L_α-phases are seen up to 15% oil in the solvent; transparent microemulsion with low viscosity is seen with 30% oil.

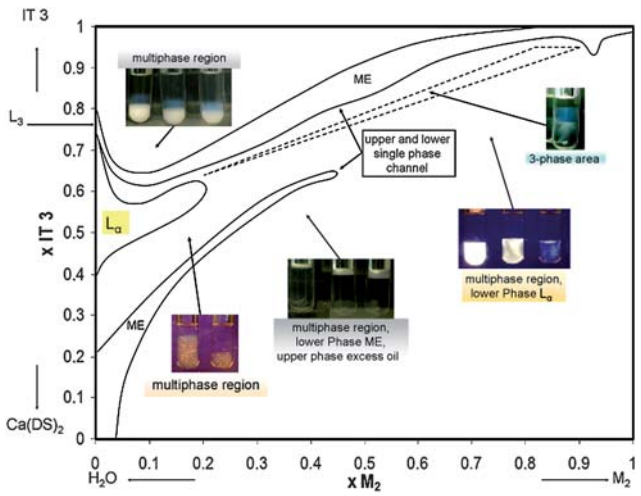

Fig. 1 Phase diagram of system $Ca(DS)_2$/IT 3–H_2O/M_2 at 15% (w/w) surfactant and 40 °C. x is the mass fraction, the abbreviation "ME" stands for "microemulsion" and indicates area of isotropic single-phase channel.

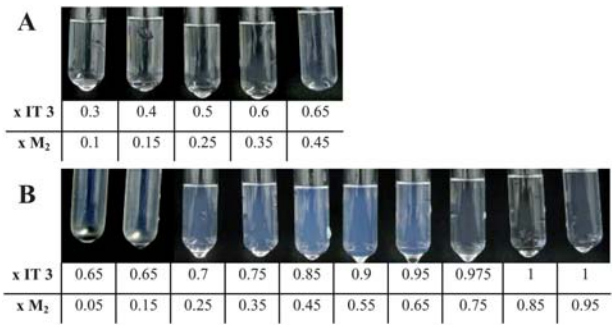

Fig. 3 Samples with 15% (w/w) surfactant mixture $Ca(DS)_2$/IT 3 at 40 °C and increasing mass fraction x of IT 3 and M_2, shown without polarisers. (A) Selected samples from lower single-phase channel. (B) Selected samples from upper single-phase channel.

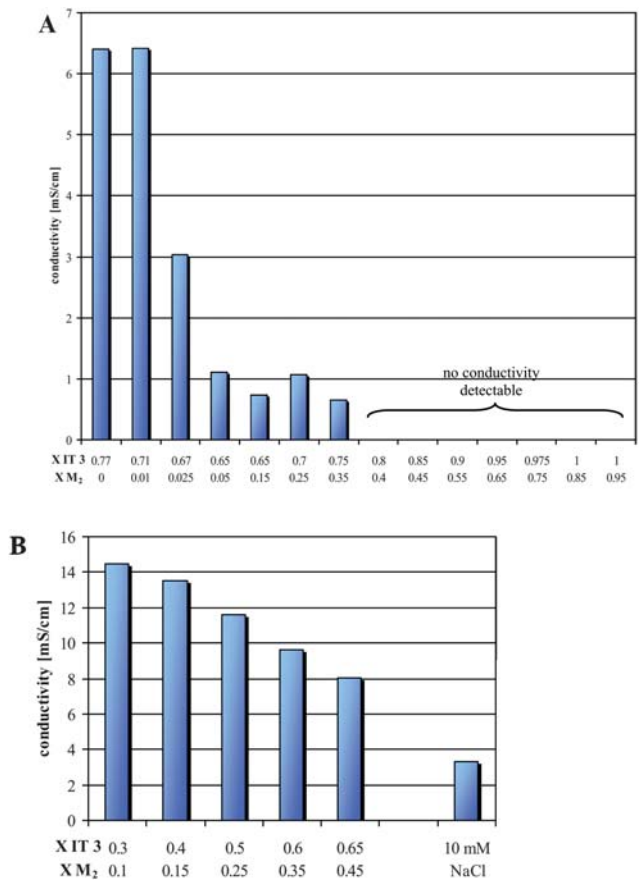

Fig. 4 Conductivity measurements in the upper (Fig. 4A) and lower (Fig. 4B) single-phase channel of the system $Ca(DS)_2$/IT 3–H_2O/M_2 at 40 °C.

in the microemulsion for the transport of the ions must be much larger than in the L_3-phase.

This means that the water channels in the ME-phase must be much smaller than in the L_3-phase where the conductivity is only about 2/3 of the value of the normal aqueous phase without surfactant. For higher mass fraction of oil, the conductivities remain about constant and drop to zero for x $M_2 > 0.35$. The complete breakdown of the conductivity means that the system changes from a bi-continuous structure to a w/o-structure. The conductivity results differ a lot from conductivity measurements on microemulsions with nonionic surfactant, in which the conductivity decreases continuously with increasing oil concentration.[13]

In many previous publications of microemulsions it was assumed that the nanostructures in the single-phase channel varied from o/w droplets to bi-continuous structures, to w/o structures.[14] The properties discussed above demonstrate that the situation in the present system must be different and more complicated.

In the following sections we show by cryo-TEM that this is indeed the case. It should, however, be clear that the situation in nonionic and in ionically charged systems may be somewhat different. Although the effect of ionic surfactants on the phase behaviour of microemulsions with nonionic surfactants already was investigated,[15] our system is the first detailed system with an ionic/nonionic surfactant mixture, for which the ionic charge was not shielded by excess salt, that forms an isotropic channel from the water side to the oil side at constant temperature.

Cryo-TEM micrographs in the upper channel

The phase diagram of this investigation was constructed with 15% surfactant. This is a high concentration to obtain high-resolution micrographs, because the bilayers are close together. It is likely that several structures are superposed in the thin film. Thus the structures are probably not as well resolved as they would be in more dilute samples.

The micrograph in Fig. 5 was prepared with 15% (w/w) surfactant with x IT 3 = 0.77, without oil and quenched from 40 °C. The micrograph shows a bi-continuous structure in which the dark lines are the folded bilayers of the L_3-phase, and the lighter grey areas are water. The thickness of the bilayers, as determined from the micrograph, is about 3 nm. The dimension of the water domains is about 10–20 nm.

As we know for sure, the direct imaging of a bi-continuous L_3-phase with a high surfactant concentration by the cryo-TEM method is very rare, but similar structures were already reported.[16]

The micrograph of Fig. 5 looks very different compared to micrographs from L_3-phases that are typically prepared with the FF-TEM technique. The most obvious difference is that in FF-TEM micrographs one observes that both the white and grey areas cover about 50% of the area while in the cryo-TEM micrographs the white area is much larger than the grey area. During preparation of the sample with the FF-technique the fracture follows the midplane of the bilayers because this is where the sample breaks most easily.[17] The result of the fracture process is a surface that is half formed from the frozen water phase and half covered by the midplane. This situation is independent from the surfactant concentration in the samples. No fracture is produced with the cryo-TEM method and the structure in the thin films is directly imaged on the micrograph. The grey and white areas reflect therefore the surfactant water ratio of the sample. In total, the three dimensional nature of the water phase

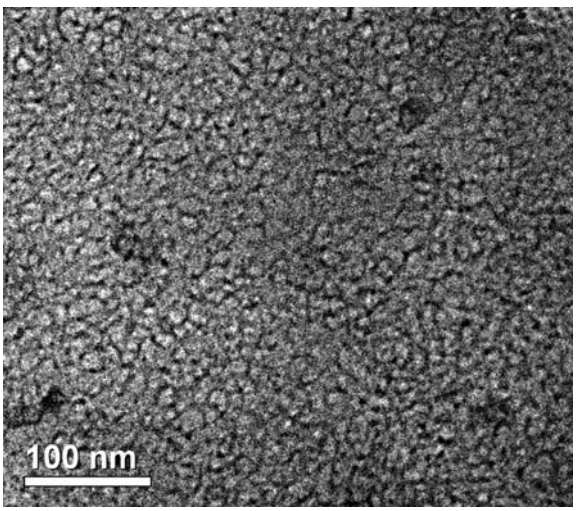

Fig. 5 Cryo-TEM micrograph of sample with 15% (w/w) surfactant $Ca(DS)_2$/IT 3, x IT 3 = 0.77, prepared at 40 °C. Micrograph shows bi-continuous network-structure of the L_3-phase.

is not so clearly seen in the cryo-TEM preparation as the three dimensional nature of the bilayer network. The cryo-TEM micrograph in Fig. 5 actually looks somewhat like a two dimensional projection of a three dimensional polyhedral foam. The L_3-phase is formed only in the very narrow composition of the samples with x IT 3 = 0.76 to 0.77. In the neighbouring L_α-phase with a composition of x IT 3 = 0.75 the structures are very different.

For comparison with the microstructure of the L_3-phase, micrographs are shown in Fig. 6 of a sample with a slightly different composition, namely with x IT 3 = 0.75.

The micrographs show the typical pattern of a L_α-phase in which the bilayers are perpendicular to the surface of the thin film (Fig. 6A). The interlamellar spacing is of the order of 10–15 nm and the bilayer thickness is about 3 nm. The micrographs of the L_3-phase and the L_α-phases are very consistent with each other. On close inspection of the micrographs of the L_α-phase one is able to see defects in some regions (Fig. 6B). These defects are indicated on the micrographs of Fig. 6B with white arrows.

One notes situations where two adjacent bilayers seem to be connected by bridges. These could be the structures that have been theoretically predicted.[18] It is noteworthy that the micrograph in Fig. 6A looks like a fingerprint with a much larger scale. It is somewhat surprising that the bilayers in the thin films are all perpendicular to the film surface. From optical microscopy, in contrast, it is known that the bilayers are very often aligned parallel to the film surface, what is known under homeotropic alignment. The reason for the different situation that is shown in Fig. 6 may be a result of the film thickness. In the holes of the polymer films the thickness of the surfactant phase varies. On parallel alignment the bilayers would have to form different numbers of bilayers at different positions in the thin film in order to keep the interlamellar distance the same. Such defects cost energy and the film might therefore prefer the perpendicular alignment.

The structures in L_α-phases with a lower IT 3 content (x IT 3 = 0.65) are somewhat different (Fig. 7).

Large multilamellar vesicles (MLVs) are now seen in which the spacing between the bilayers is much larger than in the micrograph with $x = 0.75$. The larger spacings are probably the result of applying high shear rates to the MLV during the blotting procedure.[16]

Cryo-TEM micrographs of samples with increasing amount of oil are shown in Fig. 8. The first two micrographs (Fig. 8A and B) show similar network-like structures to the micrograph of the L_3-phase without oil (Fig. 5). It is generally assumed that the L_3-phase is a symmetric phase, where the inside and outside volume of the three-dimensional tubular structure is the same. It is likely that this symmetry is lost by the solubilisation of oil, and the microemulsion is an asymmetric phase. This can be concluded from the abrupt conductivity change that occurs

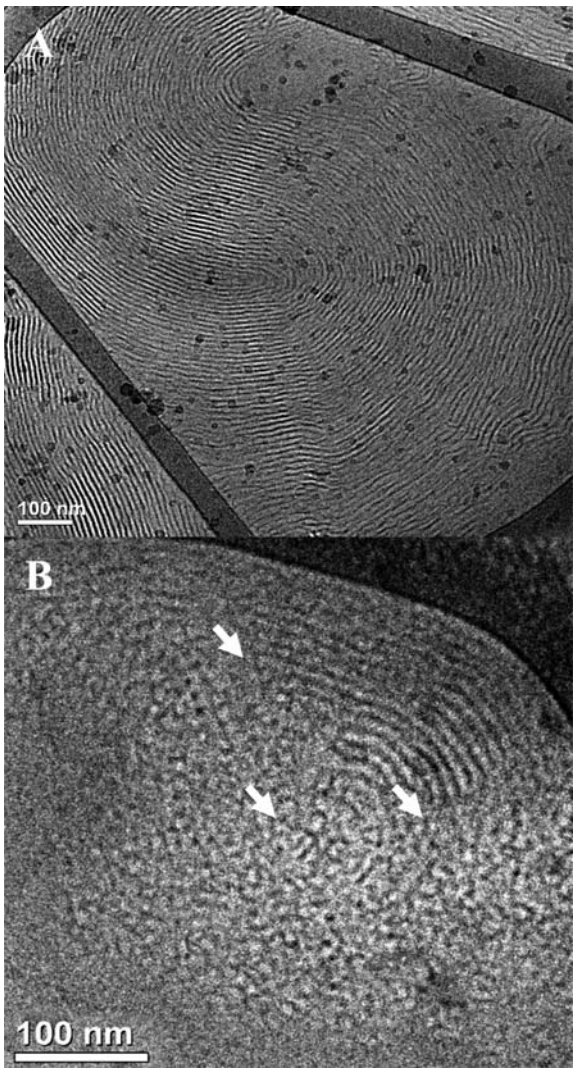

Fig. 6 Cryo-TEM of samples with 15% (w/w) surfactant $Ca(DS)_2$/IT 3, x IT 3 = 0.75, prepared at 40 °C. (A) Typical pattern of L_α-phase; (B) L_α-phase with defects, shown by white arrows.

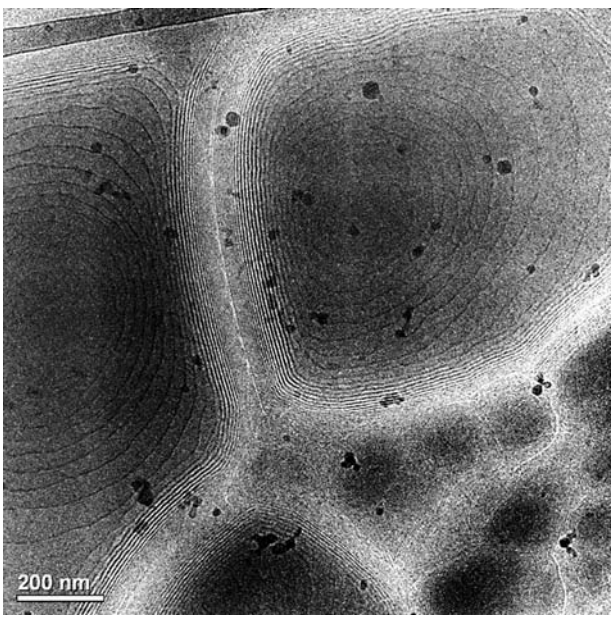

Fig. 7 Cryo-TEM image of sample with 15% (w/w) surfactant $Ca(DS)_2$/IT 3, x IT 3 = 0.65, prepared at 40 °C. Large squeezed-together multilamellar vesicles are seen.

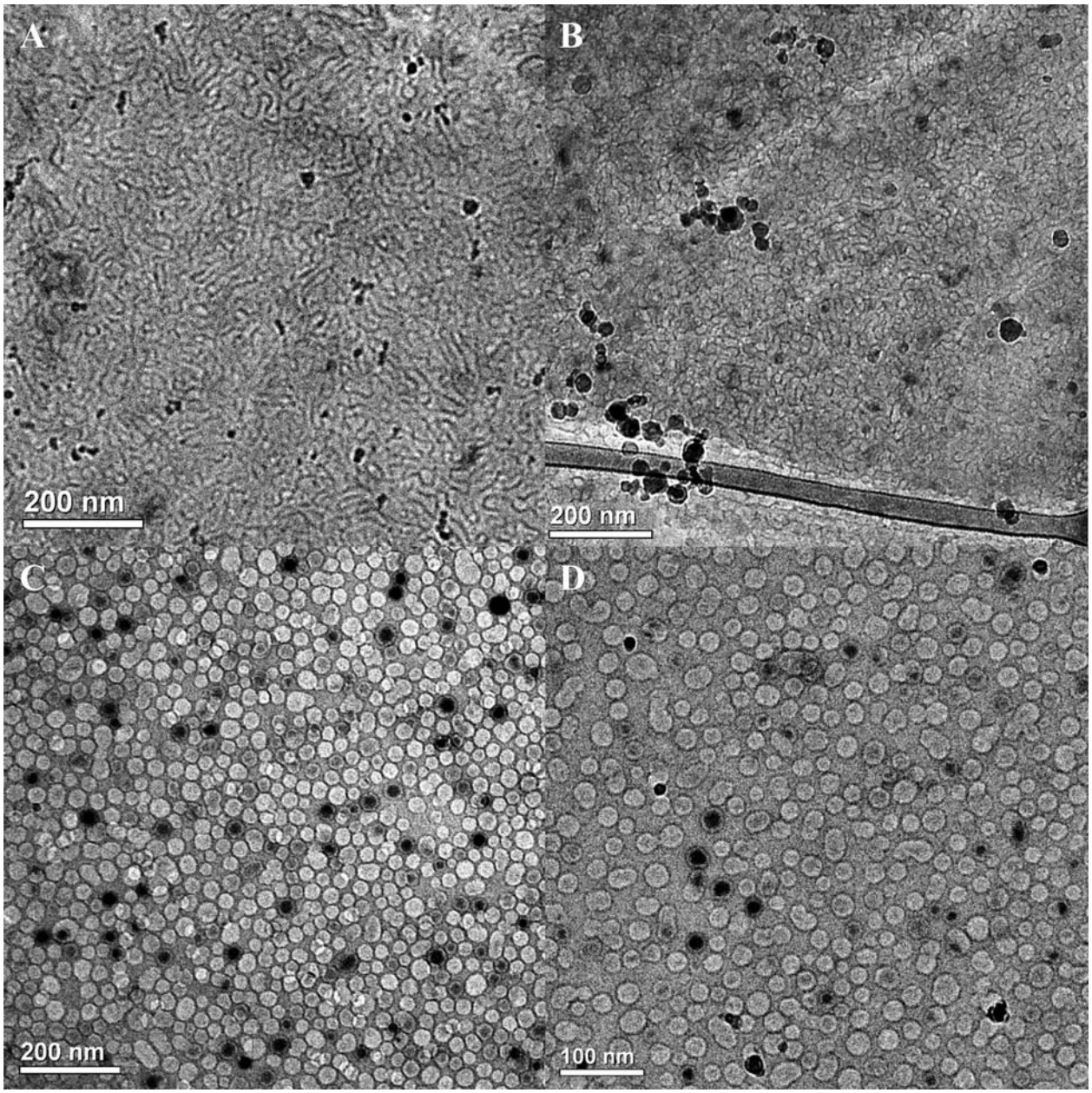

Fig. 8 Cryo-TEM micrographs of samples with 15% (w/w) surfactant $Ca(DS)_2$/IT 3, prepared at 40 °C: (A) composition x IT 3 = 0.65, x M_2 = 0.05, sponge-like structure; (B) composition x IT 3 = 0.65, x M_2 = 0.15, sponge-like structure; (C) composition x IT 3 = 0.9, x M_2 = 0.5, densely packed water droplets and (D) composition x IT 3 = 0.975, x M_2 = 0.75, less densely packed water droplets.

around x M_2 = 0.05. Indeed, the observed bi-continuous structures by the TEM micrographs of samples with solubilised oil look somewhat different from the micrographs of the L_3-phase without oil. However, some micrographs also show typical structures of L_α-phases or MLV phases. It is likely that these structures result from evaporation of M_2 in the thin film. M_2 is an extremely volatile compound. In order to decrease the evaporation as much as possible, the atmosphere in the preparation chamber had to be saturated with the microemulsion solution and the preparation had to be carried out as quickly as possible. The samples with the highest oil content (Fig. 8C and D) have different structures. In both samples globular particles are observed that are in a lighter grey than the background.

Obviously, the structure has now changed from the bi-continuous structure to w/o droplets. At 50% oil the droplets are densely packed while in the sample with 75% oil the droplet are more dispersed. The droplets have about the same size in the two samples. The diameter of the droplets varies from 20 to 30 nm. Similar globular particles already have been observed in the system AOT–*n*-decane–D_2O by FF-TEM.[19]

The micrographs with 50% and 75% oil show some interesting details that are worth emphasizing. In Fig. 8C some of the small globular particles are very dark in comparison to the light grey for most of the other droplets. These particles make up a few percent of the total number of particles. All those particles are crystalline ice, formed during the rapid cooling process. The

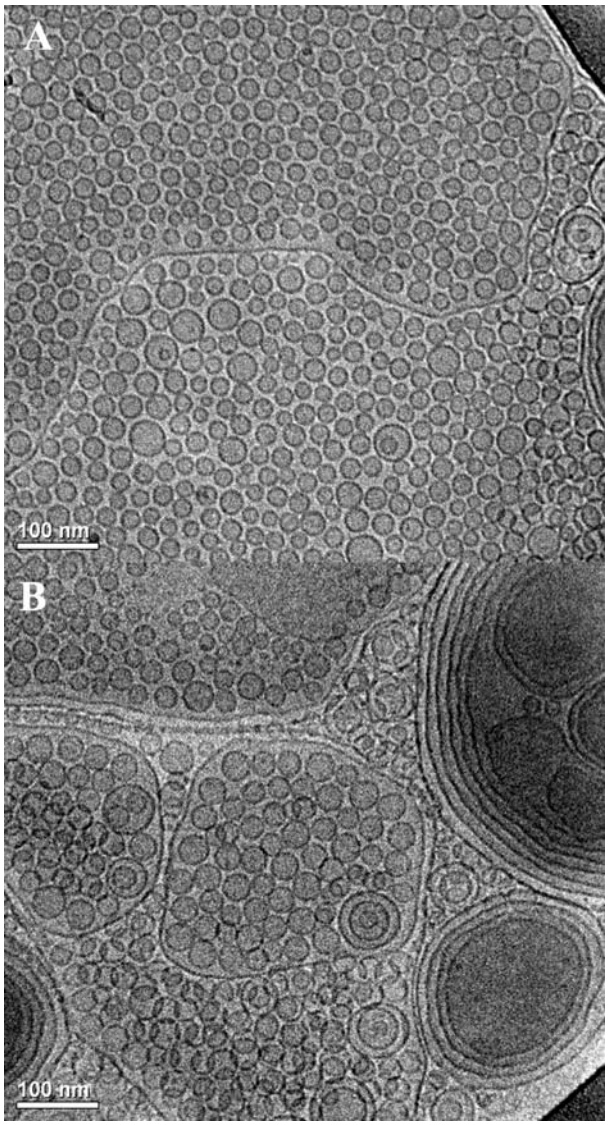

Fig. 9 Cryo-TEM micrographs of sample with 15% (w/w) surfactant $Ca(DS)_2$/IT 3, x IT 3 = 0.4, x M_2 = 0.15, prepared at 40 °C. (A) Small unilamellar vesicles with diameter from 13 to 40 nm. (B) Small unilamellar vesicles and multilamellar vesicles.

cooling rates achievable by liquid nitrogen, used here to avoid oil dissolution, are insufficient to vitrify water (but are sufficient to vitrify the oil!). Thus, the small water domains freeze into crystalline hexagonal ice. These nano-crystals are randomly oriented with respect to the electron beam, so that only a few satisfy Bragg's law for electron diffraction, and those appear dark. The ice crystals that do not diffract appear light grey. The micrographs show that the ice particles could only grow to the size of the droplets, because the droplets were not connected to surrounding droplets.

Micrographs, Fig. 8A and B, with an oil fraction of 0.05 and 0.15 seem to represent situations that are in between the L_3-phase and the microemulsion situation with 50% of oil. For both samples the crystalline ice structures are somewhat larger than the water domains. These results are in agreement with conductivity measurements in the channel, which show a transition from the conductivity of the L_3-phase to a lower conductivity at an oil content of 5%, and finally to loss of conductivity at 40% oil. The development of the structures can therefore at best to be represented by a HIPE like (High Internal Phase Emulsion) structure with varying connectivity between the water domains. In some of the micrographs one can actually observe that some of the droplets are deformed to polygonal structures. Besides the apparent polyhexagon the micrograph also shows that some of the droplets have coalesced with the neighbouring structures, and have formed larger structures. All these details demonstrate that the original droplets are very dynamic species. When the equilibrium conditions are changed, they can quickly adjust to the new conditions. In contrast to the micrograph of the sample with 50% oil, the micrograph with 75% oil shows practically no irregularities. Only very few droplets seem to have formed doublets, while the large majority of the small droplets is randomly distributed in the oil matrix. All in all, clean micrographs of a w/o-microemulsion by cryo-TEM are astonishing and rare, as it had been often assumed, that oil-rich samples cannot be imaged directly,[20] as the oil gets dissolved in the regularly used cryogen liquid ethane, or the alternative cryogen liquid nitrogen would not provide the sufficient cooling-rate to vitrify the specimen.[21]

Cryo-TEM micrographs in the lower channel

The lower single-phase channel has a large slope with increasing oil concentration. In addition, the channel is very narrow. As a result of these two conditions it is difficult to obtain good micrographs from the structures in the channel. As it is obvious from the channel, the structures in the channel could change, and the original structures are no longer in equilibrium with their surroundings, when the samples of the channel lose a few percent of oil by evaporation. This is indeed the case, as is demonstrated in Fig. 9, where two micrographs are shown that were obtained from a sample with x IT 3 = 0.4 and 15% oil. One micrograph (Fig. 9A) shows only small unilamellar vesicles with diameters ranging from 13 to 40 nm. The other micrograph (Fig. 9B) also shows uni- and multilamellar vesicles with interlamellar spacings that are consistent with the surfactant concentration of 15%.

In addition, both micrographs show long lines that separate or surround large domains of different shades. Those represent an encapsulation of small vesicles by larger ones.

Model for the calculation of the microemulsion droplet size

Dimensions for the water or oil droplets in the microemulsions can easily be calculated with the core–shell model and with the help of the oil–surfactant or water–surfactant ratio.

With the volume of the core

$$v_C = \frac{4}{3} r^3 \pi$$

and the volume of the shell which is equal to the volume of the surfactant,

$$v_S = 4\pi r^2 d$$

one obtains the simple equation

$$\frac{v_C}{v_S} = \frac{4\pi r^3}{3 \times 4\pi r^2 d} = R$$

and $r = R3d$.

In this equation d is the thickness of the surfactant monolayer, namely the thickness of the shell. The thickness d can experimentally be appreciated from the cryo-TEM micrographs of the L_α-phase or can be estimated from the number of CH_2-groups in the surfactant molecules. In an exact calculation, the different lengths of the two surfactant molecules and their different mole ratios in the upper and lower channel have to be considered.

The assumed d value, the volume ratio of the core and shell v_C/v_S, the calculated diameters $D_{cal}=2r + 2d$ of the droplets and the experimentally determined diameters D_{exp} from the cryo-TEM images are given in Table 1.

Table 1 Overview of the calculated diameters D_{cal} and experimentally determined diameters D_{exp} of the microemulsion droplets from the lower and upper single-phase channel

Size of droplets in lower channel					
x M_2	d/nm	v_C/v_S	r/nm	D_{cal}/nm	D_{exp}/nm
0.15	1.5	1.12	5	13	13–40

Size of droplets in upper channel						
x M_2	x H_2O	d/nm	v_C/v_S	r/nm	D_{cal}/nm	D_{exp}/nm
0.5	0.5	1.5	2.83	12.8	29	36 ± 6
0.75	0.25	1.5	1.42	6.4	16	25 ± 6

For the calculation of v_C/v_S, the density of the surfactant mixture was estimated to 1 g cm^{-3}, for the volume of the oil, we used the density of 0.76 g cm^{-3} for M_2.

The agreement between the calculated and experimental determined diameters in the lower channel are not very good. The micrograph of the microemulsion with x $M_2 = 0.15$ from the lower channel shows a large variety of small vesicles with diameters from 13–40 nm, which does not agree with the model.

In contrast to the lower channel, the measured size of the droplets from the upper channel differs only little from the calculated values. Although the droplets show a certain variety in size distribution, the experimental determined diameters are in good agreement with the core–shell model, considering the difficult conditions for sample preparation as the high volatility of the silicone oil and the high temperature.

Conclusion

The nanostructures in the two isotropic channels of a microemulsion of the silicone oil hexamethyldisiloxane (M_2) and a surfactant mixture of the anionic surfactant calcium dodecyl sulfate $Ca(DS_2)$ and the nonionic surfactant iso-tridecyl-triethyleneglycolether (IT 3) have been determined by cryo-TEM. Contrary to microemulsions with a pure nonionic surfactant, the channels can be formed in this system at constant temperature by adjusting the mass fraction of the two surfactants. The channel with the higher mass fraction of nonionic surfactant begins with the L_3-phase on the water side, and runs with a shallow slope to the oil side, when the mass fraction is plotted against the oil content. Conductivity results and cryo-TEM micrographs indicate that bicontinuous structures exist in this channel from the water side to a microemulsion with a 65/35 water oil ratio. The micrographs show that the structure in the bi-continuous region changes from an L_3-type structure to a HIPE-type structure. Water droplets in the oil matrix exist from the middle of the phase diagram until the oil side. This differs from the nanostructures of microemulsions with nonionic surfactants, where elements of bicontinuous microstructures, even at high oil contents, are reported.[22] The sizes of the w/o-droplets in the upper channel are consistent with simple geometrical considerations. They increase, as expected, with an increasing mass fraction of water.

The lower channel begins on the water side with an L_1-phase and reaches with increasing oil concentration to the middle of the phase diagram. The channel contains o/w droplets in a continuous water matrix. No connection was found between the two channels. Because of the high volatility of the oil, the droplets in this channel were difficult to image with the cryo-TEM method. Small vesicles were obtained in many preparations, instead of the droplets. The vesicles were obviously formed in the thin cryo-film in the time between forming and fixation by temperature quenching. Therefore, we are trying to improve the design of our CEVS to allow us work with more highly volatile solvents such as M_2, with even smaller concentration changes. We are also looking for a microemulsion system based on a lower-volatility oil, that gives a similar phase diagram.

Experimental

Materials

The nonionic surfactant iso-tridecyl-triethyleneglycolether, abbreviated as IT 3, was obtained from Sasol, Co., Hamburg (Marlipal O13/30). Sodium dodecyl sulfate (SDS, cryst. research grade) was purchased from the Serva Co., Heidelberg. $MgCl_2 \times 6H_2O$ and $CaCl_2 \times 2H_2O$ were purchased from the Grüssing Co., Filsum. The silicone oil hexamethyldisiloxane, abbreviated M_2, was purchased from the Wacker Co., München, *n*-decane was obtained from the Merck Co., Darmstadt.

Preparation of $Ca(DS)_2$ and $Mg(DS)_2$

For the preparation of $Ca(DS)_2$ and $Mg(DS)_2$, 400 mM SDS-solution were mixed with either 200 mM $CaCl_2$ or $MgCl_2$ solution under stirring. The bivalent counterions Ca^{2+} and Mg^{2+} bind stronger to the dodecyl sulfate than the sodium-ion, leading to a precipitation of $Ca(DS)_2$ in solution below its Krafft-temperature of 50 °C, and $Mg(DS)_2$ below its Krafft-temperature of 25 °C. The solutions were heated up to 60 °C for the solution with $CaCl_2$, or warmed up above 25 °C for the solution with $MgCl_2$ to obtain a clear solution, and then cooled down to 20 °C. After precipitation, $Ca(DS)_2$ and $Mg(DS)_2$ were washed several times with de-ionised water to remove excess salt. The purity of the filtered surfactant thus could be checked by measuring the conductivity of its flow through. The washed $Ca(DS)_2$ and $Mg(DS)_2$ were dried for several days in a cabinet dryer at 50 °C, and later used without further purification.

Preparation of samples

All samples were prepared by weighing in directly the components in test tubes, first surfactant and co-surfactant, H_2O, and, as last component, M_2, due to its high volatility. The test tubes were sealed with Teflon tape, tempered at 40 °C in a water bath, and vortexed several times thoroughly. All samples were incubated at least 3 days at 40 °C before being investigated for their phase behaviour. For the phase diagram, the samples below *x* IT 3 0.3 had to be prepared with $Mg(DS)_2$ instead of $Ca(DS)_2$ to avoid problems with precipitation of $Ca(DS)_2$. In general, a phase diagram was scanned with a resolution of 5% in the composition of the mass fraction of IT 3 and M_2. Finer steps were investigated in the beginning of the upper single-phase channel, and in between the two single-phase channels to find a possible connection of both channels. The multiphase samples were viewed and imaged without and in between crossed polarisers, to visualise the birefringence of lamellar regions.

Cryo-Transmission Electron Microscopy (Cryo-TEM)

The specimens for cryo-TEM were prepared in a controlled environment vitrification system (CEVS) and plunged into liquid ethane at its freezing point.[23] For oil continuous samples, the specimens were plunged into liquid nitrogen in order to overcome problems with solvent dissolution.[24] The CEVS was kept at 40 °C and the atmosphere either saturated with H_2O for the samples without oil, or directly with the investigated microemulsion solution for samples containing oil. Due to high volatility of the silicone oil, the specimens were prepared as quickly as possible. Specimens, kept below −178 °C, were examined in an FEI TI2 G^2 transmission electron microscope, operated at 120 kV, using a Gatan 626 cryoholder system. Images were recorded digitally in the minimal electron dose mode by a Gatan US1000 high-resolution CCD camera, with the Digital Micrograph software package.

Acknowledgements

We want to thank the Russell Berrie Nanotechnology Institute, Technion (RBNI), for providing us the opportunity to investigate our specimen by electron microscopy. For the excellent technical assistance, we especially thank Judith Schmidt and Dr Ellina Kesselman, and all members of the Lab of the Department of Chemical Engineering, Technion-Israel Institute of Technology, Haifa 32000, Israel.

Notes and references

1 R. Strey, *Curr. Opin. Colloid Interface Sci.*, 1996, **1**, 402–410.
2 S. J. Chen, D. Fennell Evans and B. W. Ninham, *J. Phys. Chem.*, 1984, **88**, 1631.
3 S. H. Chen and S. L. Chang, *J. Phys. Chem.*, 1991, **95**, 7427–7432.
4 C. Mathew, Z. Saidi, J. Peyrelasse and C. Boned, *Phys. Rev. A*, 1991, **43**(2), 872–882.
5 J. Bergenholtz, A. A. Romagnoli and N. J. Wagner, *Langmuir*, 1995, **11**(5), 1559–1570.
6 T. Sottmann and C. Stubenrauch, Phase Behavior, Interfacial Tension, and Microstructure of Microemulsions, in *Microemulsions: Background, New Concepts, Applications, Perspectives*, ed. C. Stubenrauch, John Wiley & Sons, Oxford, 2009, ch. 1.
7 T. Sottmann and R. Strey, Microemulsions, in *Soft Colloids V—Fundamentals in Interface and Colloid Science*, ed. J. Lyklema, Elsevier, Amsterdam, 2005, ch. 5.
8 F. Lichterfeld, T. Schmeling and R. Strey, *J. Phys. Chem.*, 1986, **90**, 5762–5766.
9 T. Sottmann and R. Strey, *J. Chem. Phys.*, 1997, **106**, 8606–8615.
10 C. Stubenrauch and T. Sottmann, Microemulsions stabilized by Sugar Surfactants, in *Sugar-Based Surfactants: Fundamentals and Applications*, ed. C. C. Ruiz, Taylor & Francis, CRC Press, Boca Raton, 2009, ch. 12.
11 IT 3 is commercially available under the name "Marlipal O13/30" from Sasol Germany GmbH, Auckelmannsplatz 1, 20537 Hamburg, Germany.
12 L. Wolf, H. Hoffmann, K. Watanabe and T. Okamoto, PCCP, submitted.
13 M. Kahlweit, et al., *J. Colloid Interface Sci.*, 1987, **118**, 436–453.
14 R. Strey, *Colloid Polym. Sci.*, 1994, **272**, 1005–1019.
15 M. Kahlweit, B. Faulhaber and G. Busse, *Langmuir*, 1994, **10**, 2528–2532.
16 D. Danino, D. Weihs, R. Zana, G. Orädd, G. Lindblom, M. Abe and Y. Talmon, *J. Colloid Interface Sci.*, 2003, **259**, 382–390.
17 H. Hoffmann, C. Thunig, U. Munkert, H. W. Meyer and W. Richter, *Langmuir*, 1992, **8**, 2629–2638.
18 R. Strey, W. Jahn, G. Porte and P. Bassereau, *Langmuir*, 1990, **6**, 1635–1639.
19 W. Jahn and R. Strey, *J. Phys. Chem.*, 1988, **92**, 2294–2301.
20 L. Belkoura, C. Stubenrauch and R. Strey, *Langmuir*, 2004, **20**, 4391–4399.
21 V. Agarwal, M. Singh, G. McPherson, V. John and A. Bose, *Langmuir*, 2004, **20**, 11–15.
22 S. Burauer, L. Belkoura, C. Stubenrauch and R. Strey, *Colloids Surf., A*, 2003, **228**, 159–170.
23 D. Danino, A. Bernheim-Groswasser and Y. Talmon, *Colloids Surf., A*, 2001, **183**, 113–122.
24 Y. Talmon, D. Danino, J. Satayavolu and R. Gupta, *J. Colloid Interface Sci.*, 2002, **249**, 180–186.

